Structure of poly(lactic-acid) PLA nanofibers scaffolds prepared by electrospinning

2014 IOP Conf. Ser.: Mater. Sci. Eng. 59 012003

(http://iopscience.iop.org/1757-899X/59/1/012003)

IOP Conf. Series: Materials Science and Engineering **59** (2014) 012003 doi:10.1088/1757-899X/59/1/012003

Structure of poly(lactic-acid) PLA nanofibers scaffolds prepared by electrospinning

E Y Gómez-Pachón[1]*, R Vera-Graziano[2], R Montiel Campos[3]

[1] Escuela de Diseño Industrial, Universidad Pedagógica y Tecnológica de Colombia-UPTC, Seccional Duitama, Carrera18 Calle 22, Duitama, Boyacá, Colombia
[2] Instituto de Investigaciones en Materiales, Universidad Nacional Autónoma de México, Avenida Universidad 3000, Delegación Coyoacán, 04510 México, D. F., México[3] Departamento de Polímeros, Universidad Autónoma Metropolitana, México D. F, México, 09340 México DF, México

E-mail: edwin.gomez02@uptc.edu.co, edwinyesidgom@yahoo.com.mx

Abstract. The structural properties of poly(lactic-acid) PLA nanofiber scaffolds prepared by electrospinning have been correlated with their process condition. The influence of the electrospinning processing parameters on structure including fiber orientation, take-up velocity and post-thermal treatment was analyzed. The structure and the properties of the scaffolds were studied by x-ray diffraction (XRD), atomic force microscope (AFM), scanning electron microscopy (SEM), high resolution transmission electron microscopy (HRTEM), and differential scanning calorimetry (DSC). The existence of crystallinity into the nanofibres of PLA was found. The careful observation by HRTEM shows an amorphous core and a semicrystalline shell structure (supramolecular), and the surface of nanofiber observed by AFM shows a laminate periodic along the main axis of the fiber. These observations will be useful in understanding the structure–property relationships of oriented nanofibre scaffolds for medical or biological applications.

1. Introduction

The use of scaffolds and porous materials produced by several techniques are more common nowadays for tissue engineering [1]. A global tendency is the use of biodegradable biomaterials, similar to native tissues, composed by fibers like collagen, which might promote the cell growth and the extracellular matrix generation [2-4]. In order to achieve this goal, several techniques have been used to obtain scaffolds such as drawing, template synthesis, phase separation, self-assembly, biocomponent extrusion and electrospinning among others. Among the several techniques to produce scaffolds, electrospinning is one of the most versatile alternatives for controlling the structural parameters of fibrous scaffolds such as diameter, texture, porosity and fiber orientation [4-7].

[1]* To whom any correspondence should be addressed.

An interesting work about the effect of crystallinity of PLA microfiber by electrical and centrifugal field on mechanical responses was described by Liao et al. [8]. Lim and Tan reported that electrospun polycaprolactone (PCL) nanofibers with smaller diameters had a higher degree of molecular orientation, crystallinity and mechanical properties [9]. In other paper, Tan and Lim reported the effect of annealing on electrospun poly(L-lactic acid) (PLLA) about crystalline structure after electrospinning [10]. They concluded that annealing was found to increase the Young's modulus of the nanofiber due to the increase in crystallinity and the change in morphology. It was clear that the fiber morphology affects the mechanical response of these materials. Wong et al. deduced an enhancement of molecular orientation and an abrupt shift in the elastic modulus of electrospun PCL occurred at around 700 nm in diameter [11].

Naraghi et al. studied the effect of diameter of polyacrylonitrile (PAN) nanofibers about the improvement of molecular orientation and mechanical properties [12]. Their results pointed out that molecular orientation is created at the late stages of the electrospinning process when the polymer jet viscosity increases and bending instabilities take place. Baji et al. also reported the influence of electrospinning parameters on the morphology and microstructure of several nanofibers (PLA, PCL, polyoxymethylene, nylon, cellulose acetate and other materials) and, in consequence, on their mechanical properties [13]. Yoshioka et al. studied the structure of polyethylene (PE) fibers by transmission electron microscopy (TEM) and the fiber structure was related to the fiber diameter. Therefore, they proposed three different structural models 1) the random-oriented crystalline 2) the shish-kebab and 3) the fibrillar structure [14].

Inai et al. have carried out tensile tests of single electrospun PLLA nanofibers collected in a rotating disc at different take-up velocities (tangential velocity produced by the rotating drum or disc) and found an improvement on the mechanical properties. Also, they reported the effects of the conductivity of the solution and the polymer concentration on the structure of PLLA electrospun [15]. Arinstein et al. suggested that nanofibers have a supramolecular structure composed by different phases [16]. Cicero et al [17] studied fibers of PLA produced by two-step melt-spinning. They found that structural properties can be widely manipulated through a combination of draw ratio and temperature. Using AFM, the fiber morphology as found to be highly fibrillar.

In our perspective there are fundamental issues about the internal fiber structure that must be taken into account such as the hierarchical structure. It has been suggested [16-18], but not clearly proven, that electrospun nanofibers can be visualized as composite materials, because they ~~likely~~ present an amorphous core and a supramolecular (semicrystalline) shell.

The internal structure and morphology of nanofibers of PLA has not been determined with enough precision because the nanometer dimensions. This work focuses on the effects of the velocity take-up and annealing on the microstructure of nanofibers of PLA. These experimental studies about microstructure of nanofiber of PLA and scaffolds structures was supported by a plausible inference of the experimental evidence from X-ray diffraction (XRD), differential scanning calorimetry (DSC), atomic force microscopy (AFM), scanning electron microscopy (SEM), high resolution transmission electron microscopy (HRTEM).

2. Materials and methods

Poly(lactid acid) of Mw 230000 (NatureWorks 2002D LLC, MN USA) was dissolved in 2, 2, 2-trifluoroethanol (Sigma Aldrich) to obtain a 16 % w/v of PLA solution, using magnetic stirring. The PLA solution was electrospun to obtain both random and uniaxial oriented nanofiber scaffolds by using two different types of collector systems separately. The electrospinning process was performed at room conditions, at a flow rate of 0.6 ml/h and at an applied voltage of 15kV (Power supply Spellman, USA) and a digitally controlled pump (KD Scientific, USA). The collector for the random scaffolds was a 10 cm square aluminum plate. The collector to obtain oriented nanofibers is an aluminum cylinder custom-designed that rotate at a predetermined velocity in the range of 1 to 10000 RPM, providing tangential velocities (take-up velocities) ranging between 1 to 3142.6 m/min (52.36

m/s). The nanofibers were collected at 1100 m/min and 1217 m/min (18.3 m/s and 20.28 m/s, respectively). Subsequently, the electrospun scaffolds were kept in desiccators at room temperature. Some scaffolds were annealed at 80 °C during 10 hours (Scorpion Scientific, A-50980 oven). The annealing temperature was selected based on the crystallization temperature of as-spun aligned nanofibers (around 70°C). In general, annealing takes place at any temperature between the crystallization and the melting point.

The scaffolds structure was analyzed by X-ray diffraction, XRD, (Siemmens D-500, Cu Kα radiation; λ=1.5406 Å), differential scanning calorimetry, DSC, (2910, TA Instruments), scanning electron microscopy, SEM, (JEOL-JSM-7600F), atomic force microscopy, AFM, (Nanoscope III, Digital Instruments), and high resolution transmission electronic microscopy, HRTEM, (JEOL-2100f). ImageJ software was used to measure the mean diameter of the nanofibres and the orientation of the uniaxially aligned nanofibers (ANs). SEM images (10000 X) at two different locations of each sample were obtained. The diameters of the continuous fibers located at the foreground plane of the micrograph were measured. For the statistical analysis, at least eight points per nanofibre were selected to measure the diameters. The names and abbreviations of the electrospun fibers are shown in the Table 1.

The internal transverse structure of the oriented nanofibres was observed by HRTEM (JEOL-2100f). The samples were embedded in an epoxy resin Epon-812 (Microscopy ScienceR) and cured for 3 days, to impede the fibers from flexing during the cutting process, which was carried out in an Ultracryo Microtome RMCR model MT- 7000. A conventional cutting pyramid was prepared, and fine sections (80-nm-thick) were obtained by means of a diamond blade (DIAMONTR) at room temperature, as the Tg for PLA is 60 °C. To obtain the proper contrast for the HRTEM observations, the samples were placed in a chamber under Ru04 vapour for 4 h.

Table 1. Names and abbreviations of the electrospun fibers

Names	Abbreviation
Uniaxially aligned nanofibers	AN
Uniaxially aligned nanofibers collected at 1100 m/min	$AN_{1100\ m/min}$
Uniaxially aligned nanofibers collected at 1217 m/min	$AN_{1217\ m/min}$
Annealed uniaxially aligned nanofibers	A-AN
Annealed uniaxially aligned nanofibers at 1100 m/min	A- $AN_{1100\ m/min}$
Annealed uniaxially aligned nanofibers at 1217 m/min	A- $AN_{1217\ m/min}$
Randomly oriented nanofibers	RON
Annealed randomly oriented nanofibers	A-RON

The surface of the ANs was observed by AFM (Nanoscope III, Digital Instruments) with a tip model TESP (Si) in the frequency range of 325–382 kHz (Veecoprobes). All images were taken in tapping mode and presented as height and phase images. The samples, 5x5 mm^2, were cut and fixed at the standard AFM sample holder (metal disc). To avoid displacement and mechanical vibration of the nanofibres during the tip movement, a group of a few ANs was approached, and the AFM scan rate was kept below 0.3 Hz.

3. Characterization

The purpose of the characterization was to determine the structure and morphology of the PLA nanofibers and scaffold.

3.1 External morphology of electrospun nanofibers.

A set of SEM micrographs of PLA electrospun scaffolds is shown in the Figure 1. The degree of orientation of the AN nanofibers was analyzed at two take-up collection velocities; 1100 m/min (AN 1100 m/min) and 1217 m/min (AN 1217 m/min). The Figure 1A and 1B show that almost all nanofibers are aligned along the tangential direction of the cylindrical rotating collector. Both the diameter and degree of alignment of the nanofibers were measured by mean of the software: Image J. The average deviation angle of alignment was around +/- 3 degrees. Therefore, it could be assumed that the nanofibers are uniaxially oriented. The average diameter of AN 1100 m/min nanofibers were 643.8 +/- 50 nm, they showed a high degree of nanofiber orientation (Figure 1A) with smooth and homogeneous surfaces (Figure 1B). Randomly oriented nanofibers RON scaffolds had a greater average diameter: 992 +/- 257 nm (Figure 1C) and the nanofibers showed a rough surface with considerable variation in the diameter along the longitudinal axis (Figure 1D). It can be concluded that the quality of the AN nanofibers is better than RON scaffolds. The rotational collector not only orients the nanofibers but also stretches them to a regular diameter and surface.

The influence of take-up velocity and annealing in the diameter of the nanofibers is depicted in Figure 1E. The RON (zero take-up velocity) presented the highest diameters and standard deviations. The AN $_{1100m/min}$ and AN $_{1217m/min}$ without thermal treatment had diameters of 643 +/- 50 nm and 747 ±117 nm, respectively. These results were compared with those obtained by Inai et al. [15] with AN of PLA collected at 6 m/min and 630 m/min, these had average diameters of 890+/-190 nm and 610+/- 50 nm respectively. It is worth to notice that Inai's experimental electrospinning parameters were different from ours, however, despite of the combination of parameters such as polymer concentration, feed rate, solution electroconductivity, take-up velocity, and type of collectors used in their experiments were different, the AN nanofiber diameters in both works are similar at velocities above 630 m/min. According to our results take-up velocities above 1100 m/min did not influence the nanofiber diameters. In contrast Inai et al. [15], showed that from 6 m/min to 630 m/min (10 fold change in velocity) there is a significant effect in the reduction of the nanofibers diameter.

The annealed AN nanofibers (A-AN) showed the lowest diameter average values. The A-AN $_{1100\ m/min}$ showed an average diameter of 562.8±210, while A-AN $_{1217\ m/min}$ showed an average diameter of 525.8+/- 90.4 nm. By comparing the annealed and non-annealed nanofiber it was found a small decrement in diameter, ranging between 12 and 30% as shown in Figure 1E. This behavior is due the self-assembly of the chain molecules into the nanofiber as a result of annealing. However this effect was not observed in RON.

The figure 2A shows a phase AFM image of AN prepared without annealing at a take-up velocity of 1217 m/min. Two well-defined alternating (periodic) dark and bright regions appeared on the electrospun nanofiber surface. The dark and bright regions correspond to lamellar and amorphous phases, respectively. Two different phases were clearly identified by using the phase AFM image, captured in tapping mode. This could be due to the difference in the sample hardness, density into the aligned nanofiber. Different regions of the sample were analysed by AFM with highly reproducible results. In the annealed samples, these observed features disappeared. Clearly this observation prove the assumption of Ciceron et al. [17] that represented the morphology of PLA microfibers, produced by melt spinning, as a schematic microfibrillar morphology and confirmed that this model can be used in nanofibers. The lamellar fraction $\mathbf{V_2}$ was experimentally measured by AFM and digital image analysis (Image J software), showing an average lamellar volume fraction of 35.7% for AN $_{1217m/min}$.

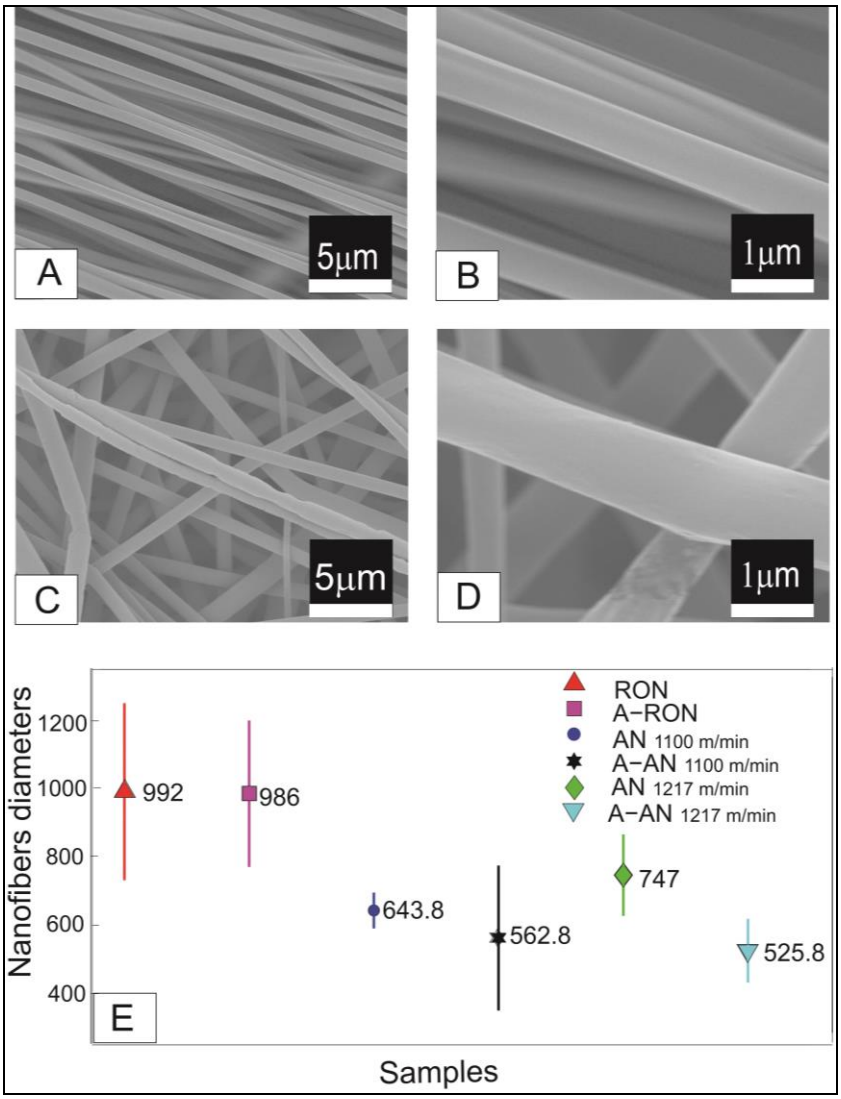

Figure 1. SEM images of electrospun PLA of nanofibers (A) Aligned nanofibers collected at 1100 m/min speed, (B) Same image at higher magnification showing a smooth surface without pores or defects, (C) Random oriented nanofibers collected in a static square plate, (D) Same image at higher magnification showing pores and defects on the surface and (E) Diameters of the different types of PLA nanofibers [random oriented (RON), annealed random oriented (A-RON), (AN) aligned (A-AN) annealed aligned] showing that size was influenced by alignment and heat treatment [18].

The HRTEM image of an AN cross-section, prepared at a take-up velocity of 1217 m/min, is displayed in the figure 2 B, where an amorphous core (bright region) and supramolecular shell (dark regions) phases are clearly distinguished. This confirms the assumption of Arinstein et al. [16] regarding the formation of oriented polymeric chains (supramolecular structure) in the shell due to the electrospinning process. Until this moment, this figure 2B is the first observation of the hierarchical structure of AN that shows the core-shell morphology. As shown in the figure 2A the shell is composed of a supramolecular lamellar phase.

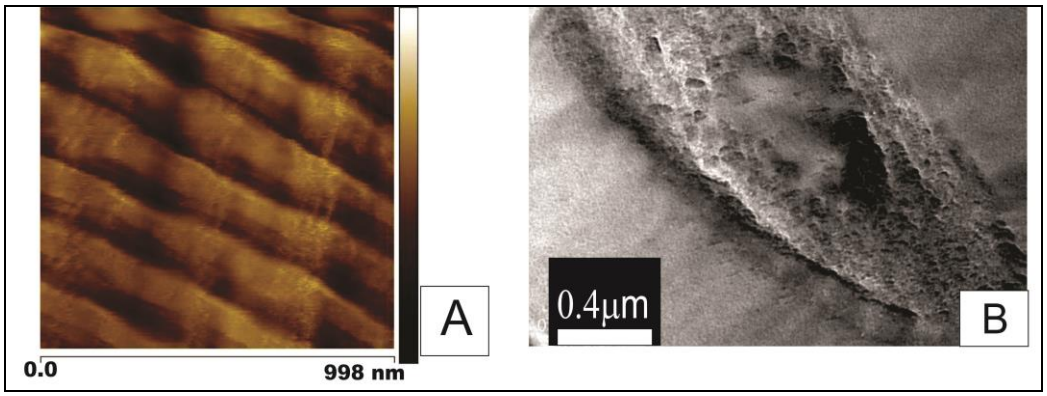

Figure 2. Structure of an aligned PLA electrospun nanofiber (A) Phase AFM image of the nanofiber surface and (B) HRTEM micrograph of the cross section of the nanofiber.

3.2 Crystallographic analysis

The XRD plots (Figure 3) suggest that the level of atomic organization of PLA is strongly dependent on the processing conditions. Bulk PLA, used as a reference, has a semicrystalline structure (purple plot line in Figure 3A) with two characteristic peaks at 16.8° and 19.2° (Bragg angles), in good agreement with those reported by Inai, et al. [15]. These results suggest a crystalline orthorhombic structure (according to PDF-2-2006 card number 00-054-1917, Diffract Plus 2005), with the following lattice parameters a=10.61, b=6.05 and c=28.8 Å. The randomly oriented nanofibers (RON) have a typical amorphous structure (green plot line in Figure 3A). The fast solidification of the fibers during the electrospinning process limited the long-period three-dimensional order at the atomic level of the PLA; therefore, no evidence of extensive crystallization was found. However, after the fibers were annealed below the melting point (A-RON) a peak at 16.8° appears (red plot line in Figure 3A). This result is a clear evidence of the self-assembly of the polymer chains at the atomic level.

Figure 3B shows the XRD results of uniaxially aligned nanofibers (AN). There is no evidence of crystallinity in AN $_{1100\ m/min}$ and AN $_{1217\ m/min}$ as depicted by the blue and black plot lines. However, as it could be expected, annealing promotes extensive crystallization of the polymer chains as shown in the red and green plot lines, where again in both plots the peak is observed at 16.8º. These results are similar to those presented by Inai, et al. [15].

It is most likely that during the electrospinning, the AN polymer chains are oriented along the main axis of the nanofibers due to both the electrical field and winding at high speeds. However, the fast solidification rate tends to inhibit crystallization of the polymer. Annealing promotes chain self-assembly and, as expected, the uniaxially oriented nanofibers (AN) develop more crystallinity than the randomly oriented nanofibers (RON).

3.3 Thermal transitions

The thermal transitions of the electrospun nanofibers were studied by DSC in order to measure crystallization trends. The thermal transitions of the electrospun nanofibers are shown in Figure 3C and 3D. It can be observed that the glass transition (Tg) and melting (Tm) temperatures are about the same in all cases: Tg=60 °C and Tm=147 °C. However, the crystallization temperature (Tc) was affected by the take-up velocity. Figure 3C corresponds to bulk PLA, RON and A-RON samples. In this case the RON and A-RON samples, showed an enthalpic relaxation due to the rapid solidification rate during electrospinning. This enthalpic relaxation temperature occurred at about 65°C (endothermic peak). As expected, the degree of molecular disorder of the chains is higher in RON than in A-RON as shown by the enthalpy values of 6.3 J/g and 5.8 J/g, respectively.

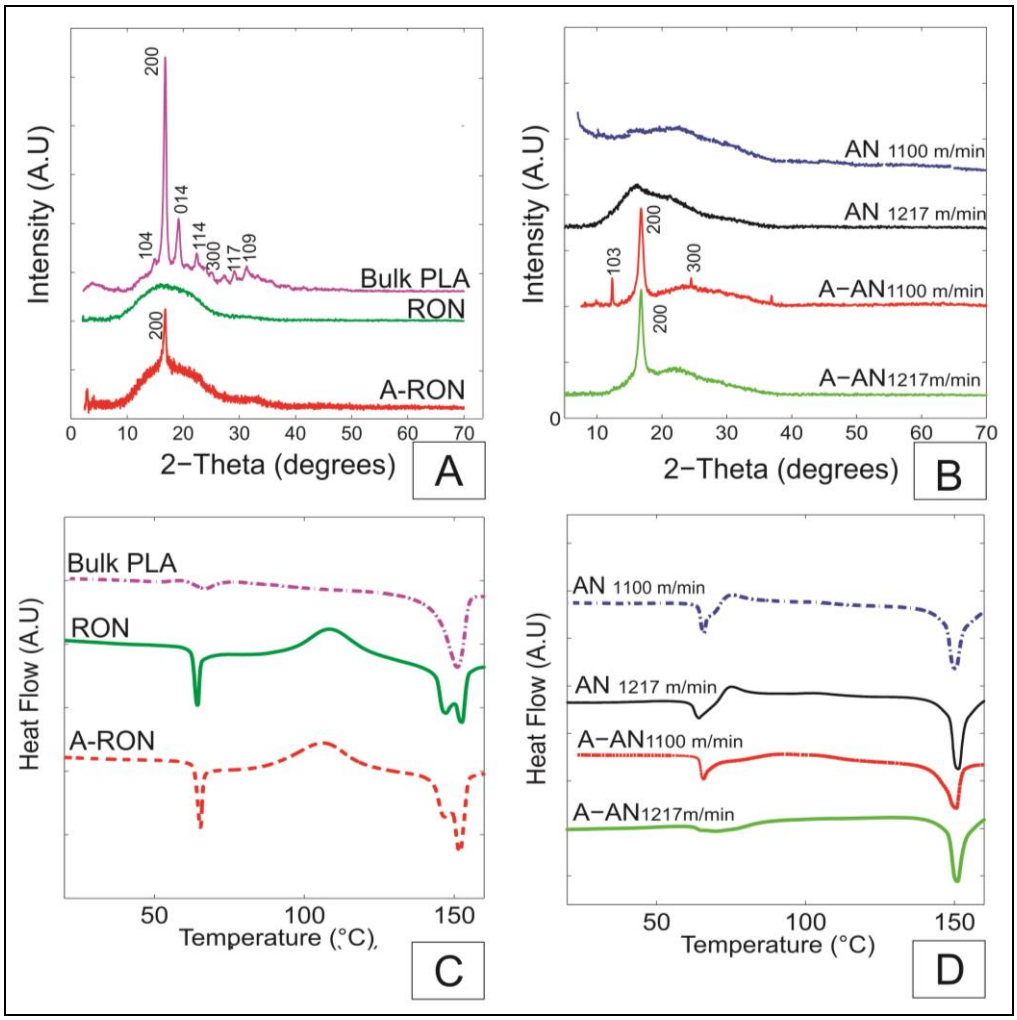

Figure 3. XRD and DSC plots of PLA nanofibers (A) Diffractograms of bulk PLA, RON and A-RON nanofibers, (B) Diffractograms of AN and A-AN nanofibers, (C) DSC of bulk, RON and A-RON nanofibers and D) DSC of AN and A-AN nanofibers [18].

It can be observed in Figure 3C that RON and A-RON plot lines show exothermic peaks between 106-108°C. These peaks, with enthalpy values of 19.4 and 23.1 J/g, respectively, correspond to the crystallization of the polymer. The energy released during crystallization is higher in A-RON because of the effect of annealing at 80°C. Melting is observed at about 147°C. Again the melting peak of A-RON is more intense than in RON with enthalpies values of 25.67 and 21.20 J/g respectively, indicating a greater crystalline fraction in A-RON fibers. The double melting point in RON may be due to two phases coexisting in the nanofibers, because the stretching during the fast electrospinning process may transforms some α crystals into the β form, that possible disrupting the lamellar packing [19].

The thermograms of AN and A-AN also show the enthalpic relaxation peaks again at about 65°C, with enthalpy value of 5.8 J/g for both AN $_{1100\ m/min}$ and AN $_{1217\ m/min}$. This value was similar than that observed in RON. After annealing, the relaxation enthalpies were smaller than in A-RON as follows: 5.8 for A-RON, 4.5 for A-AN $_{1100\ m/min}$ and 3.6 J/g for A-AN$_{1217m/min}$. This tendency was also a confirmation that the combination of take-up velocity and annealing parameters improved the internal organization of the polymer nanofibers. The AN also showed crystallization: in the case of AN $_{1100m/min}$ the crystallization peak was found at 75.3 °C with an enthalpy of 3.9 J/g, while in AN $_{1217\ m/min}$ it was at 74.8 °C with an enthalpy of 4.6 J/g. The orientation of the nanofibers by the effect of the rotational collector induced a significant change in crystallization with respect to RON nanofibers: a reduction of

about 30 °C in crystallization temperature (Tc) and smaller crystallization enthalpies, with respect to RON. It implies that AN requires less energy to reach the crystalline state.

The A-AN $_{1100m/min}$ show a Tc= 92.6°C with an enthalpy of 1.5 J/g and A-AN$_{1217\ m/min}$ did not show the crystallization peak. This shows that A-AN reached the maximum value of crystallinity after annealing. The obtained data indicate that annealing has a strong effect on both the crystallization temperature and the crystalline structure of PLA nanofibers. The melting temperatures of AN and A-AN were 146 and 148°C, respectively. The enthalpy values of AN $_{1100\ m/min}$ (28.63J/g) and AN $_{1217\ m/min}$ (31.93 J/g) are greater than those observed in A-RON (25.67 J/g) and RON (21.20 J/g), indicating that AN and A-AN are more crystalline due to the orientation of the polymer chains along the nanofibers.

In the case of A-AN the melting enthalpy was greater for the fibers collected at 1217 m/min than those collected at 1100 m/min. In A-AN $_{1100\ m/min}$ and A-AN $_{1217\ m/min}$ the enthalpies were of 18.47 J/g and 29.84 J/g, respectively. These values indicate that a higher take-up velocity improved crystal formation. Our results showed the crystallization peak, and the XRD analysis confirmed the amorphous-crystalline structure in the samples, as it can be observed in Fig. 3. The electrospinning, nanofiber orientation, take-up velocity, and annealing promote self-assembly of the polymer chains.

According to the evidence of XRD (Figure 3A and 3B), apparently AN nanofibers are not crystalline before annealing. However DSC reveals a crystallization peak in the same type of samples. The XRD technique is not the best to detect the small polymer crystalline structures in the nanofibers in contrast to DSC. In addition to the fact that DSC is a very sensible technique to detect enthalpy changes including crystallization. During the DSC experiments, the heating process induced the oriented polymer chain structures to form bigger crystals before the melting point.

Conclusions

The morphology of scaffolds of electrospun PLA nanofibers depend strongly on the take-up velocity and annealing conditions; winding the electrospun nanofibers in the rotational collector produced highly aligned nanofibers (AN). The morphology of AN was more homogeneous in diameter, without defects, because of nanofiber stretching, than those observed in randomly oriented nanofiber (RON) scaffolds. Fiber stretching produced in turn a high degree of self-assembly.
Molecular orientation increases with take-up velocity; however, the fast solidification occurring during electrospinning limited the size of the crystalline structures. Annealing promoted better molecular self-assembly in the nanofibers, increasing the size of the crystals and the degree of crystallization. Aligned nanofiber scaffolds have a hierarchical core-shell structure where the core is amorphous and the shell has a supramolecular morphology as observed by HRTEM. The surface of nanofibers has two periodic phases: the lamellar and amorphous as observed by AFM.

The morphological and structural features found in the nanofiber scaffolds allow to confirm the structures proposed by other researchers with clear and convincing evidence. Also allow to generate a complete description of the structure of the PLA nanofibers and their relationship with variables such as nanofiber orientation on scaffolding, take-up velocity of the collector and subsequent heat treatments to the spun fibers.

Acknowledgments

The authors thank Nikola Batina and Israel Morales Reyes for AFM analysis, Omar Novelo Peralta for SEM analysis, Patricia Castillo Ocampo for TEM analysis, Adriana Tejeda Cruz for XRD analysis, Damaris Cabrero Palomino for DSC analysis, Alfredo Maciel and Francisco Sanchez for the review of this paper. This project has been supported by ICyTDF (Grants 180/2009 and PICSA12-204), DGAPA-UNAM (Grants IN116809 and IN108913), CONACYT (Grant 129658 and a scholarship), PCeIM-UNAM and DIN-Dirección de Investigaciones-UPTC (Grants SGI 1397/2013) for other supports.

Reference

[1] Barnes CP, Sell S A, Boland E D, Simpson D G, Bowlin G L 2007 *Nanofiber technology: designing the next generation of tissue engineering scaffolds* Advanced Drug Delivery Reviews 59, 1413–1433.

[2] Jayaraman, K., Kotaki, M., Zhang, Y., Mo, X., Ramakrishna, S., 2004. *Recent advances in polymer nanofibers.* Journal of Nanoscience and Nanotechnology 4, pp. 52–65.

[3] Agarwal S and Wendorff J H, Greiner A 2008 *Use of electrospinning technique for biomedical applications*. Polymer 49 pp.5603–5621.

[4] Lannutti J, Reneker D, Ma T, Tomasko D and Farson D 2007 *Electrospinning for tissue engineering scaffolds*. Materials science and engineering c 27 504–509.

[5] Liao S, Murugan R, Chan C K and Ramakrishna S 2008 *Processing nanoengineered scaffolds through electrospinning and mineralization suitable for biomimetic bone tissue engineering*. *J*ournal of the mechanical behavior of biomedical materials 1, pp. 252–260.

[6] McClure M, Simpson DG and Bowlin GL 2012 *Tri-layered vascular grafts composed of polycaprolactone, elastin, collagen, and silk: Optimization of graft properties*. Journal of the Mechanical Behavior of Biomedical Materials 10 pp. 48–61.

[7] Reneker DH and Yarin A L 2008 *Electrospinning jets and polymer nanofibers.* Polymer 49 pp. 2387-425.

[8] Liao C-C, Wang C-C and Chen C-Y 2011 *Stretching-induced crystallinity and orientation of polylactic acid nanofibers with improved mechanical properties using an electrically charged rotating viscoelastic jet.* Polymer 52 pp. 4303-4318.

[9] Lim C T, Tan E P S and Ng S Y 2008 *Effects of crystalline morphology on the tensile properties of electrospun polymer nanofibers*. App. Physics Letters 92 141908-3.

[10] Tan EPS, Lim CT., 2006. *Effects of annealing on the structural and mechanical properties of electrospun polymeric nanofibres*. Nanotechnology 17 pp. 2649–2654.

[11] Wong S-C, Baji A and Leng S 2008 *Effect of fiber diameter on tensile properties of electrospun poly(ε-caprolactone)*. Polymer 21 pp. 4713–4722.

[12] Naraghi M, Arshad S N and Chasiotis I 2011 *Molecular orientation and mechanical property size effects in electrospun polyacrylonitrile nanofibers* Polymer 52 pp. 1612-1618.

[13] Baji A**,** Mai Y**,** Wong S**,** Abtahi M and Chen P 2010 *Electrospinning of polymer nanofibers: Effects on oriented morphology, structures and tensile properties* Composites Science Technology 70 703-718.

[14] Yoshioka T, Dersch R, Tsuji M and Schaper A K 2010 *Orientation analysis of individual electrospun PE nanofibers by transmission electron microscopy*. Polymer 51 pp. 2383-2389.

[15] Inai R, Kotaki M and Ramakrishna S 2005 *Structure and properties of electrospun PLLA single nanofibres*. Nanotechnology 16 pp. 208–213.

[16] Arinstein A, Burman M, Gendelman O and Zussman E 2007 *Effect of supramolecular structure on polymer nanofibre elasticity*. Nature nanotechnology 2 pp. 59–62.

[17] Cicero J A and Dorgan J R 2002 *Physical Properties and Fiber Morphology of Poly(lactic acid) obtained from continuous two-Step melt spinning* Journal of Polymers and the Environment 9, pp. 1-17.

[18]Gomez-Pachon E, Sánchez-Arévalo F M, Sabina F J, Maciel-Cerda A, Campos M R, Batina N, Morales-Reyes I and Vera-Graziano R 2013. *Characterisation and modelling of the elastic properties of poly(lactic acid) nanofibre scaffolds*. Journal of Materials Science 48, pp. 8308-8319.

[19] Montes De Oca H and Ward I M. *Structure and Mechanical Properties of Poly(L-lactic acid) Crystals and Fibers*. Published online in Wiley InterScience (www.interscience.wiley.com).